STUDY OF LIGHT NEUTRON-RICH NUCLEI VIA ONE-NEUTRON KNOCKOUT REACTIONS

Carme Rodríguez Tajes*, for the S245 collaboration

V Encuentro de Física Nuclear, septiembre 2010

Universidade de Santiago de Compostela

* present address: Centro de Láseres Pulsados (CLPU)

Introduction

Nuclear structure studies have advanced on the basis of a well-established shell-structure associated with certain magic numbers.

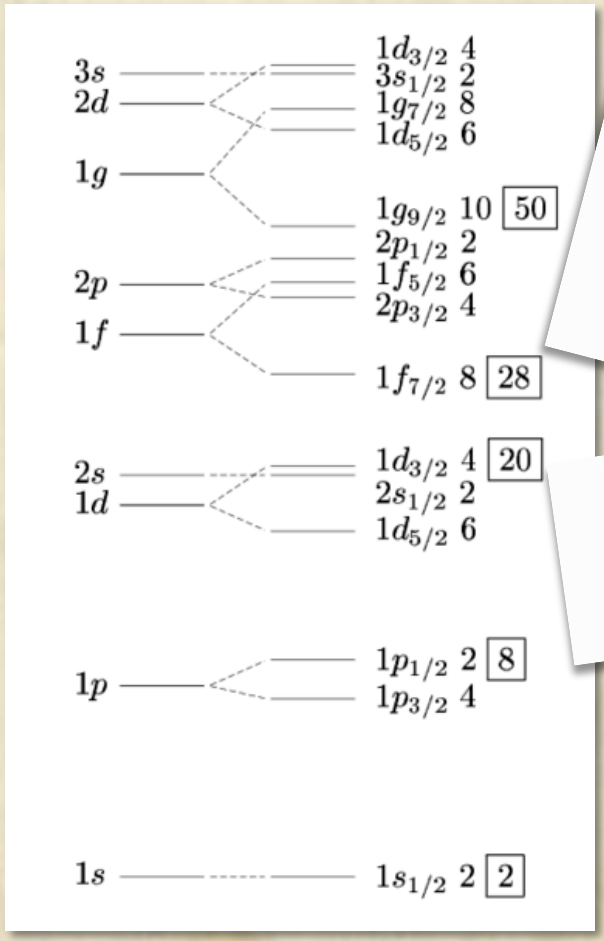

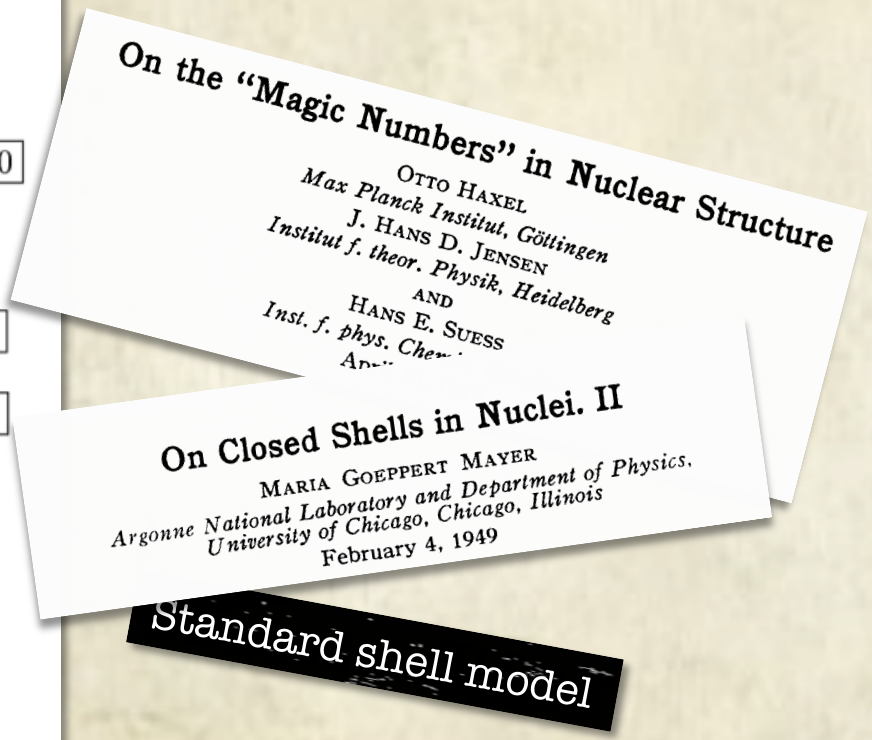

Radioactive-beam facilities opened the door to the experimental research far off β stability, where unexpected phenomena appear...

Nuclear halos

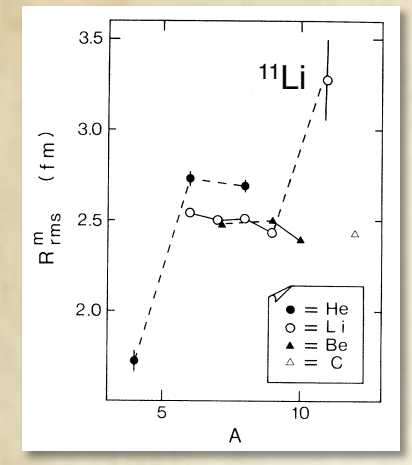

Tanihata et al., Phys. Rev. Lett. 55 (1985) 2676

Island of inversion

Thibault et al., Phys. Rev. C 12 (1975) 644

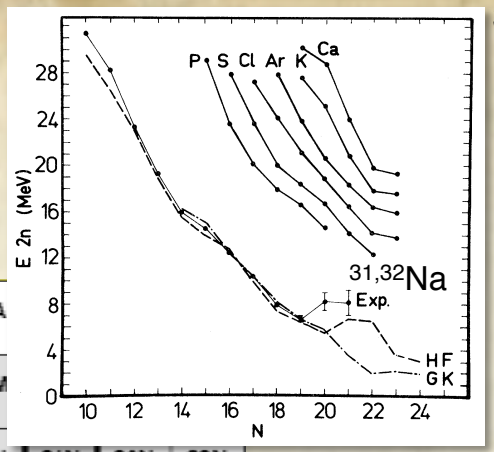

Otsuka et al., Phys. Rev. Lett. 87 (2001) 082502

Changes in magic numbers

One-neutron knockout reactions

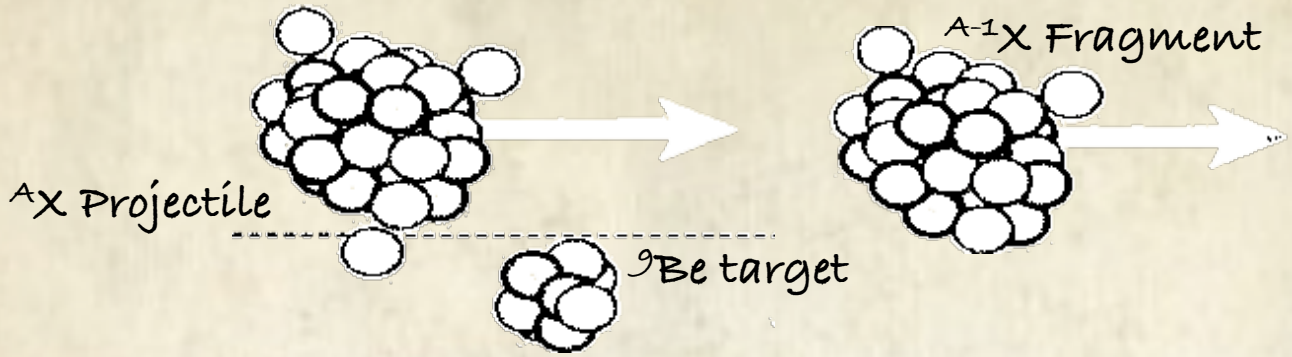

Stripping is the relevant process at high energies (transparent limit of the Serber model).

Exclusive measurements

$$\text{Projectile} = \sum C^2S\left[\text{core} \otimes \text{neutron}\right]$$

γ-ray detectors gave rise to exclusive measurements that made possible to distinguish the states of the A-1 fragment.

$$\sigma_{th}(I^\pi) = \sum C^2S(I^\pi, nlj)\sigma_{sp}(I^\pi, nlj)$$

measured

theory

It is possible to determine spectroscopic factors, $C^2S(I^\pi, nlj)$.

Longitudinal momentum distributions

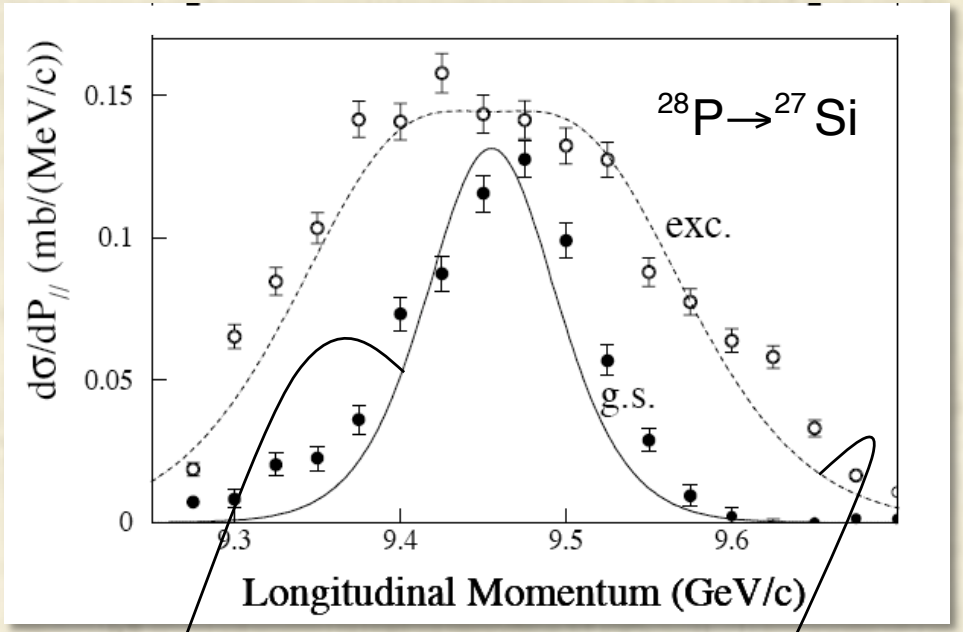

Navin et al., Phys. Rev. Lett. 81 (1998) 5089.

The longitudinal momentum distributions of the A-1 fragment reflect the orbital angular momentum of the nucleon removed in the reaction.

Experimental setup at the FRS spectrometer

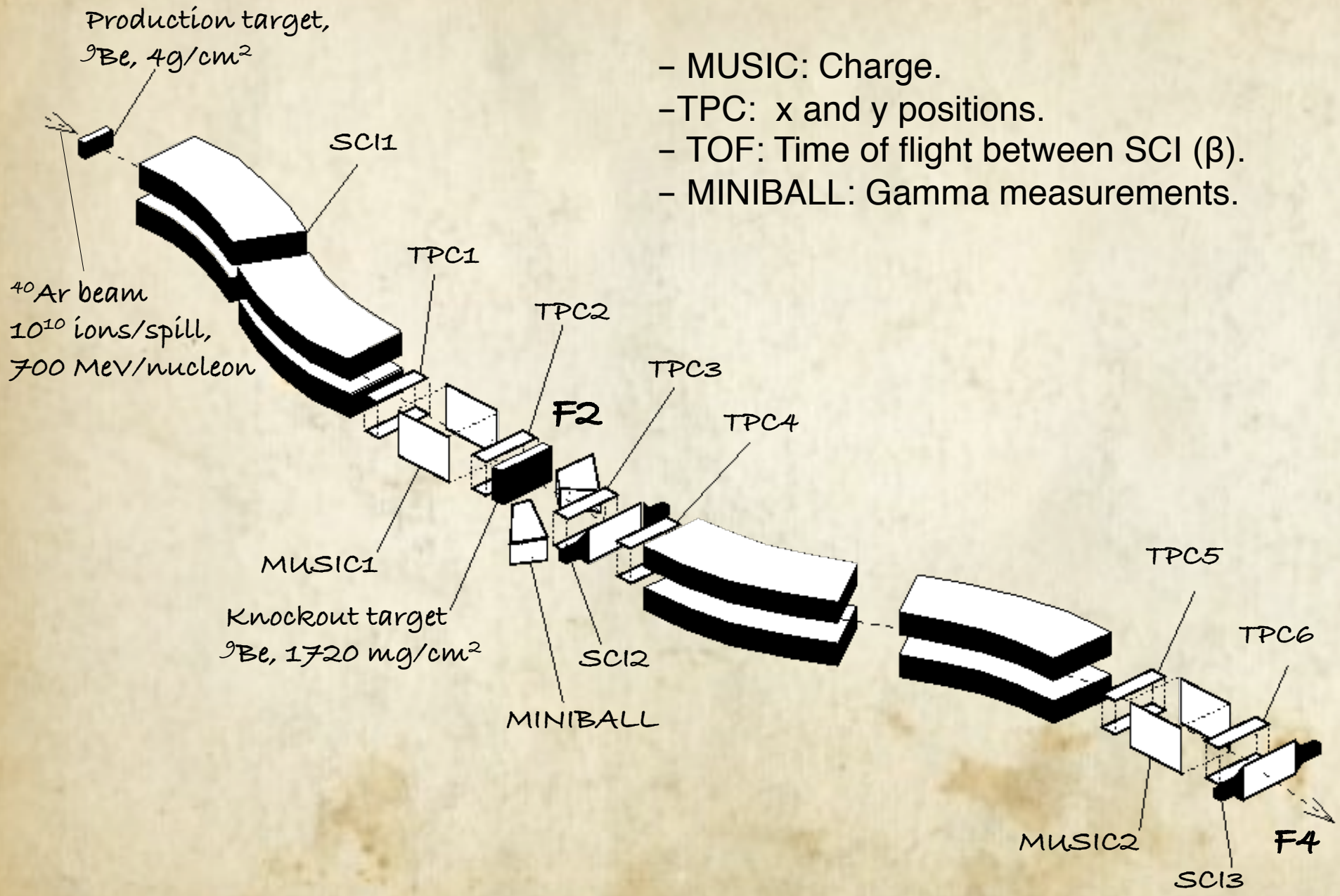

- MUSIC: Charge.
- TPC: x and y positions.
- TOF: Time of flight between SCI (β).
- MINIBALL: Gamma measurements.

Identification

Identification of projectiles and knockout fragments from measurements of the charge and A/Z ratio.

TOF

$$B\rho = \gamma\beta c\left(\frac{m_0}{q}\right)$$

positions at TPCs

Identification plots were used to calculate the cross-section:

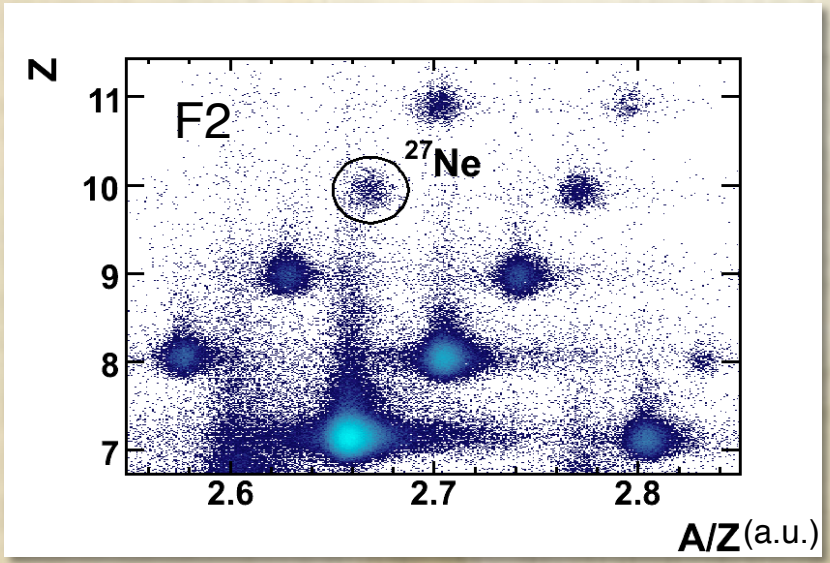

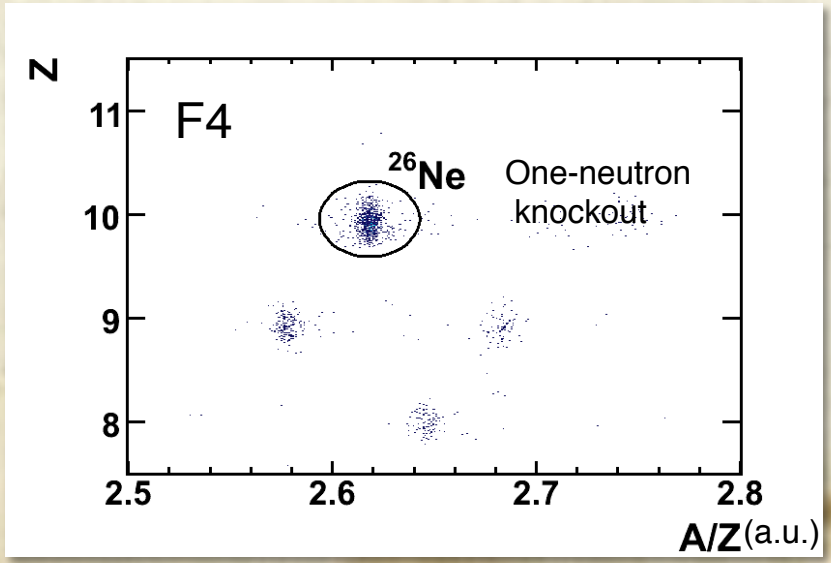

Calculation of the longitudinal momentum

The energy loss in the target region is translated in a position change at F4.

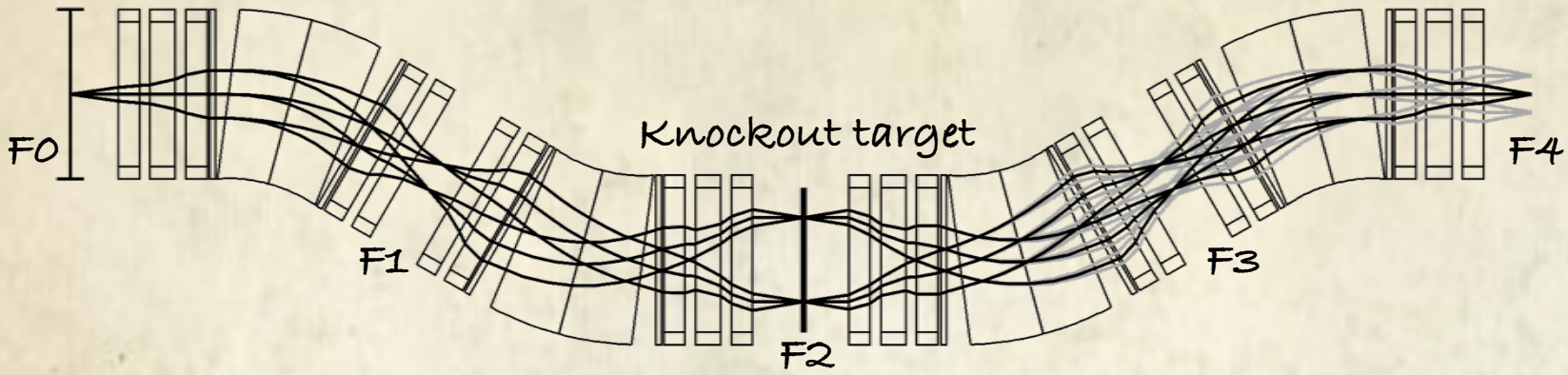

The longitudinal momentum is calculated from the transfer matrix of the FRS:

$$p_f = q_f B\rho_{S2,4}\left(1+\frac{x_{F4}}{D_{S2,4}}+\frac{x_{F2}}{D_{S0,2}}\right)$$

It is converted to the reference frame of the projectile:

$$p_{//} = \gamma_{proj}\left(p_f - \beta_{proj}\frac{E_f}{c}\right)$$

γ measurements with MINIBALL

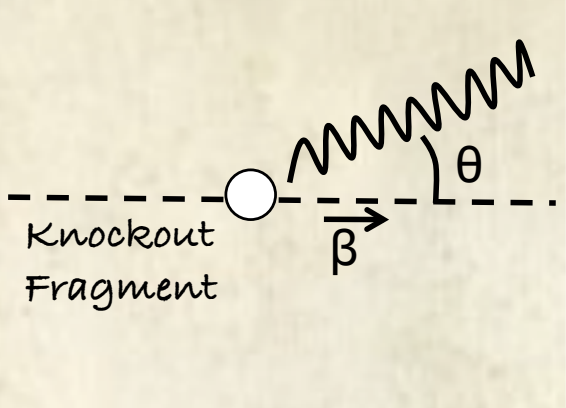

MINIBALL (8 cluster of 3 segmented Ge crystals).

Reconstruction of the γ-ray energy:

$$E_{lab,cluster} = \sum E_{core}$$ Addback

$$E_{source} = \gamma E_{lab}\left(1+\beta\cos\theta\right)$$ Doppler correction

Results

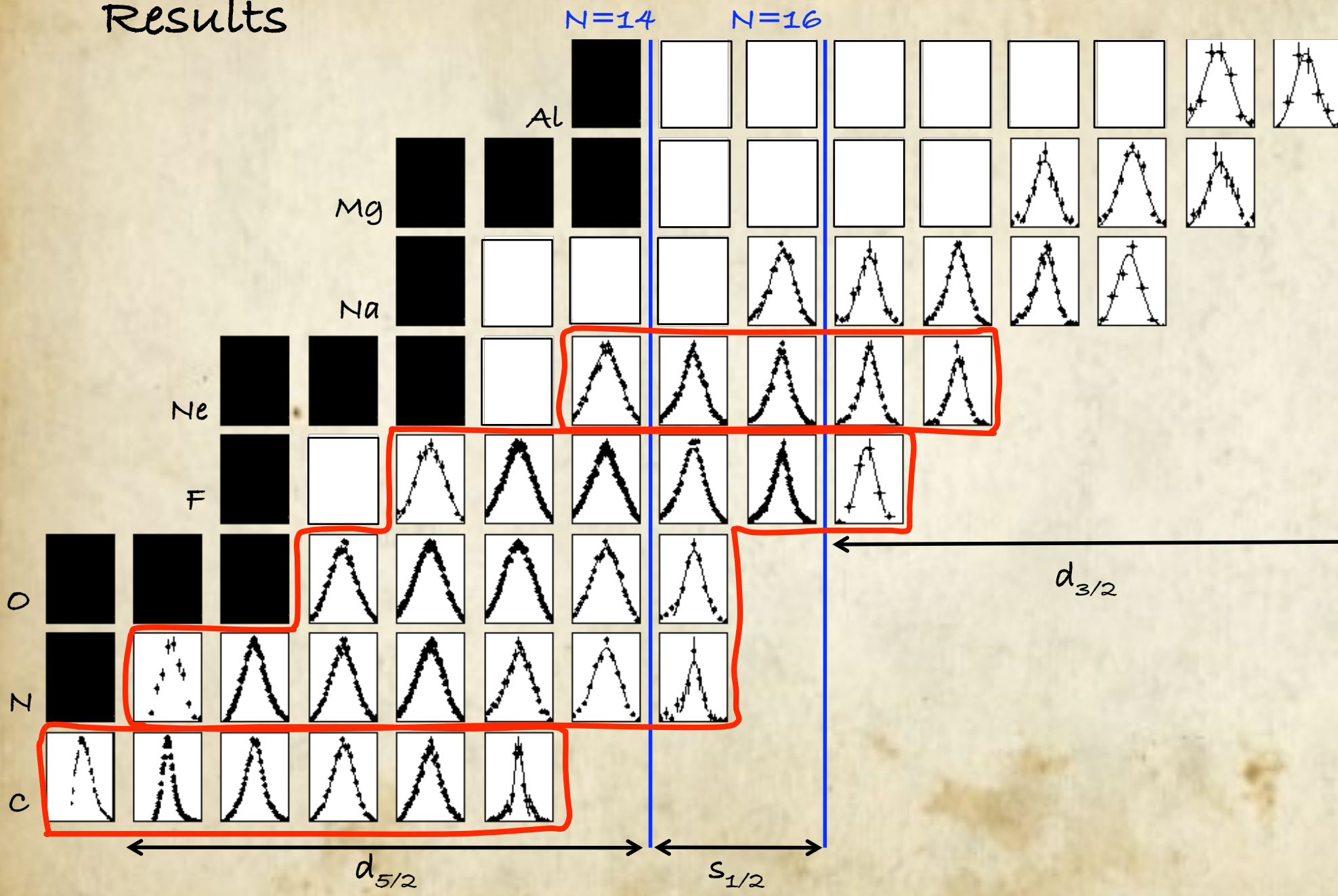

C. Rodriguez-Tajes et al., Phys. Rev. C 82 (2010) 024305.

Results for $^{14-19}$C isotopes

Odd-mass C isotopes are good candidates for neutron-halo configurations.

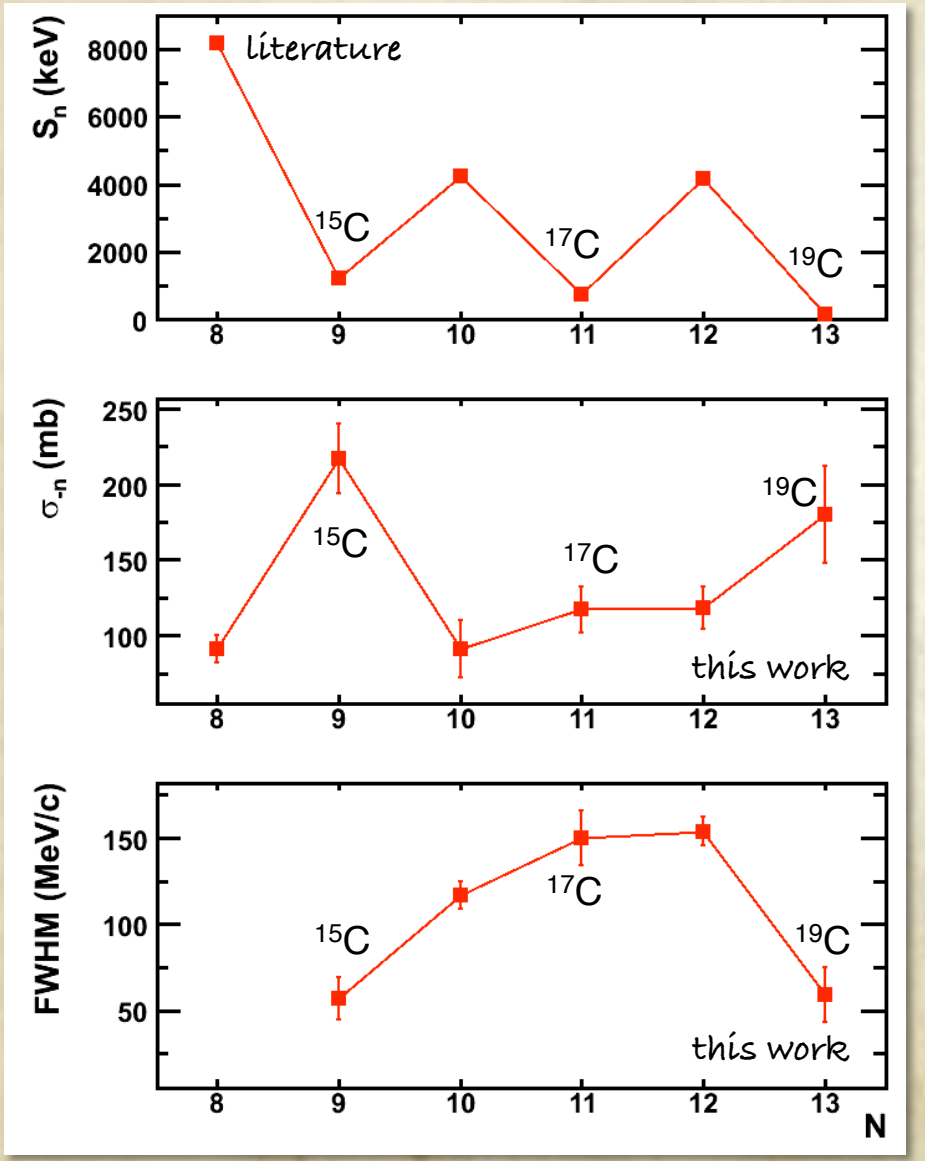

^{15}C: $2s_{1/2}$ intruder configuration.

^{17}C: Halo supression caused by a $l=2$ configuration.

^{19}C: One-neutron halo structure and $l=0$ valence neutron.

γ measurements in ^{17}C one-neutron knockout

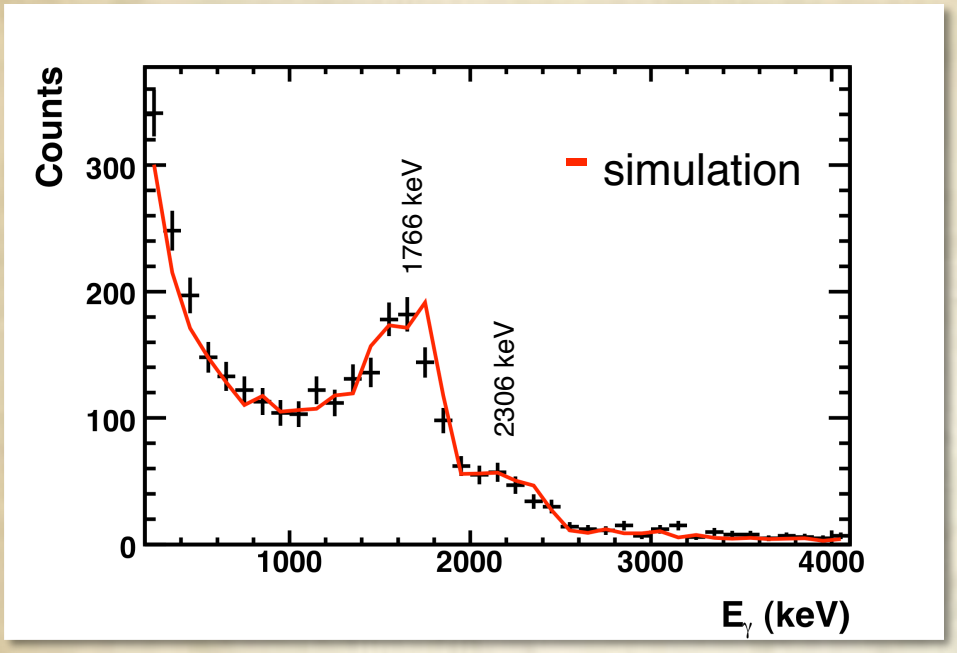

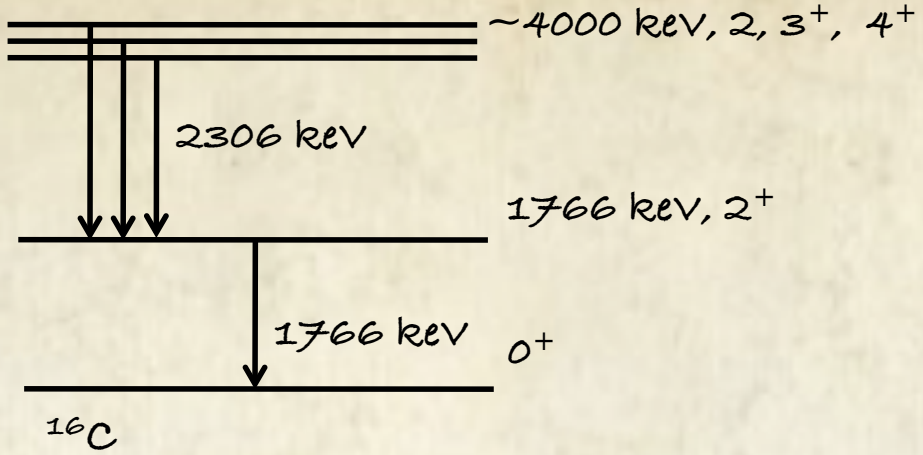

Contribution from the ^{16}C ground state in disagreement with the 2% predicted by shell-model calculations.

I^π	E (keV)	σ_{-n} (mb)	b
0^+	0	27 ± 8	0.32 ± 0.08 0.19 ± 0.09 (i)
2^+	1766	36 ± 9	0.48 ± 0.04 0.52 ± 0.08 (i)
$2, 3^+, 4^+$	~4000	21 ± 5	0.25 ± 0.04 0.29 ± 0.05 (i)

$^{16}C(2^+) \times d_{3/2}$

(i) Maddalena *et al.*, Phys. Rev. C 63 (2001) 024613.

Results for $^{16-22}$N, $^{19-23}$O and $^{21-26}$F isotopes

N, O and F isotopes exhibit significant $s_{1/2}$ admixtures when crossing N = 14.

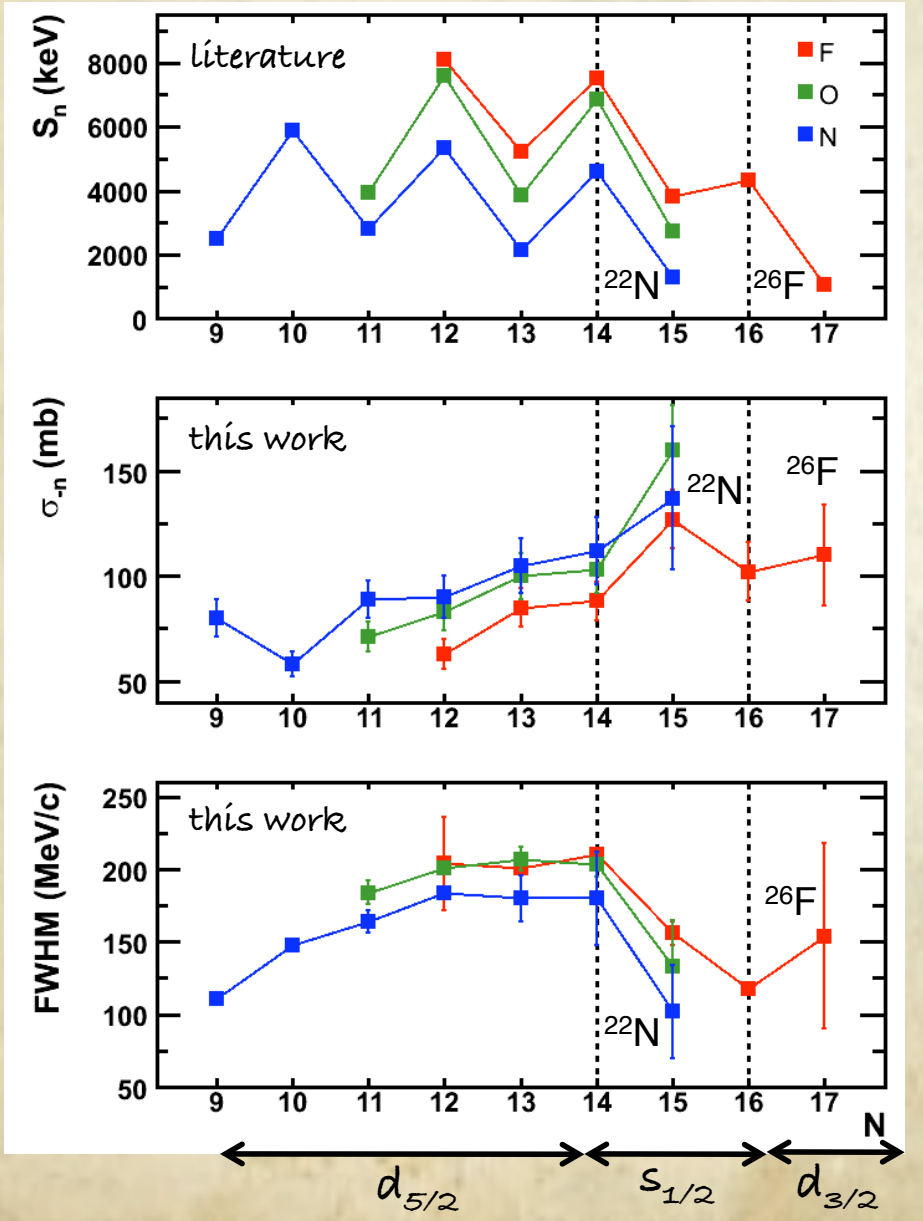

^{22}N: First one-neutron knockout data

^{26}F: Possible $2s_{1/2}$ neutron coupled to an excited state of ^{25}F, as suggested by Fernandez et al., PhD thesis.

γ measurements in ^{19}N one-neutron knockout

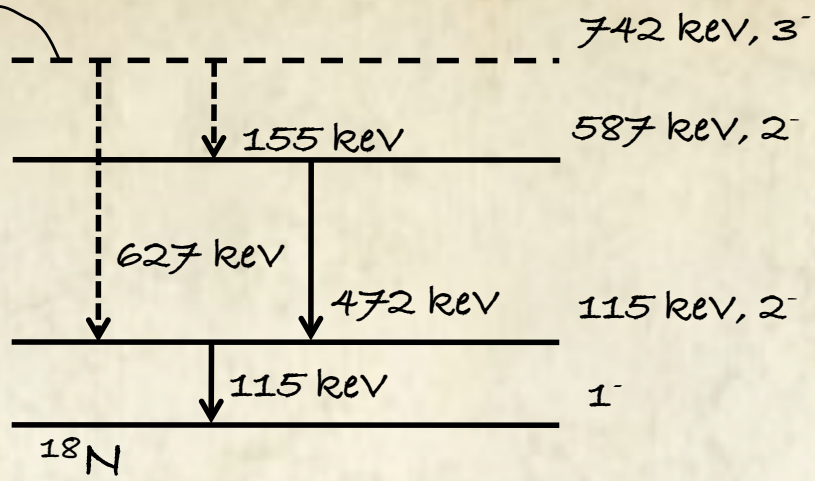

Wiedeking et al.
Phys. Rev. C 77 (2008) 054305.

Three clear peaks, at 143, 472 and 615 keV, observed in this experiment.

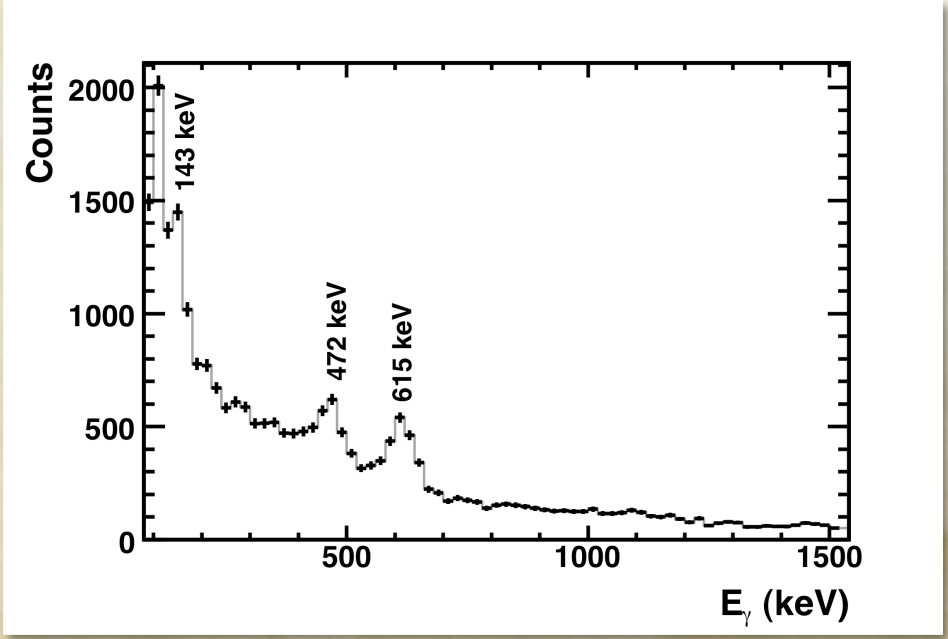

Decay scheme in agreement with Wiedeking et al., limits for the branching ratios were obtained.

Results for $^{24-28}$Ne isotopes

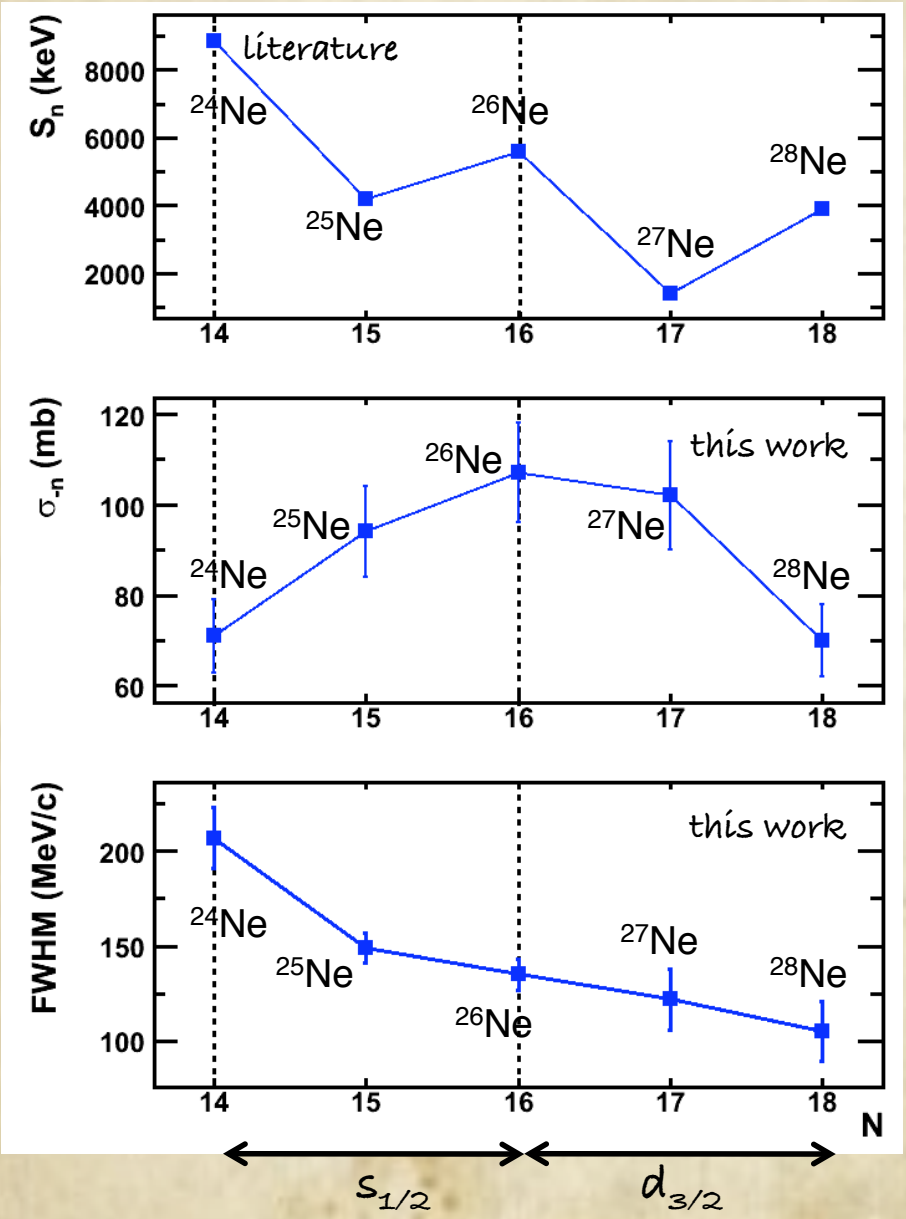

^{24}Ne: $d_{5/2}$ configuration.

$^{25-26}$Ne: $s_{1/2}$ admixtures at N=15, 16.

$^{27-28}$Ne: The valence neutron occupies a $s_{1/2}$ level, rather that $d_{3/2}$.

Analysis of the momentum distributions

Momentum distributions determined by the asymptotic form of the wave function.

$$\psi_{lm}(\vec{r}) \rightarrow \text{Hankel functions}$$

Analytical solutions for the lowest angular momenta: $\frac{dN_{l=0}}{dk_z}, \frac{dN_{l=1}}{dk_z}, \frac{dN_{l=2}}{dk_z}$

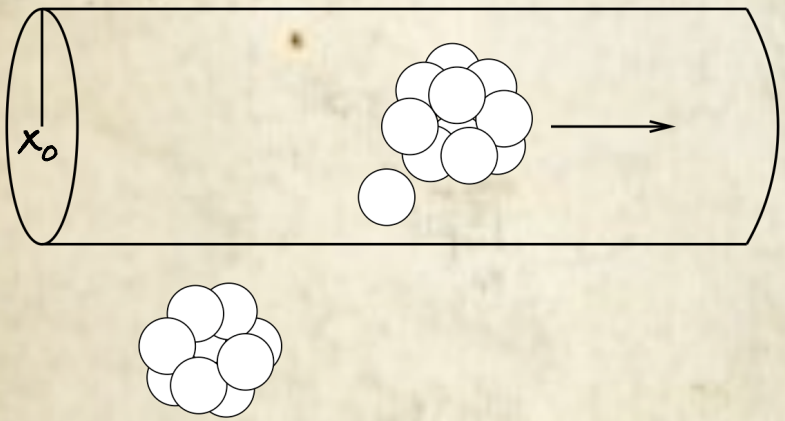

Depend on the neutron separation energy (S_n) and a lower cut-off on the impact parameter (x_o).

$$Proj = W_{gs}(core \otimes n)_{gs} + W_{exc}(core \otimes n)_{exc} \Rightarrow \frac{dN}{dk_z} = W_{gs}\left(\frac{dN_l}{dk_z}\right)_{gs} + W_{exc}\left(\frac{dN_l}{dk_z}\right)_{exc}$$

$W_{gs,\,exc}$ = weigth of the configuration

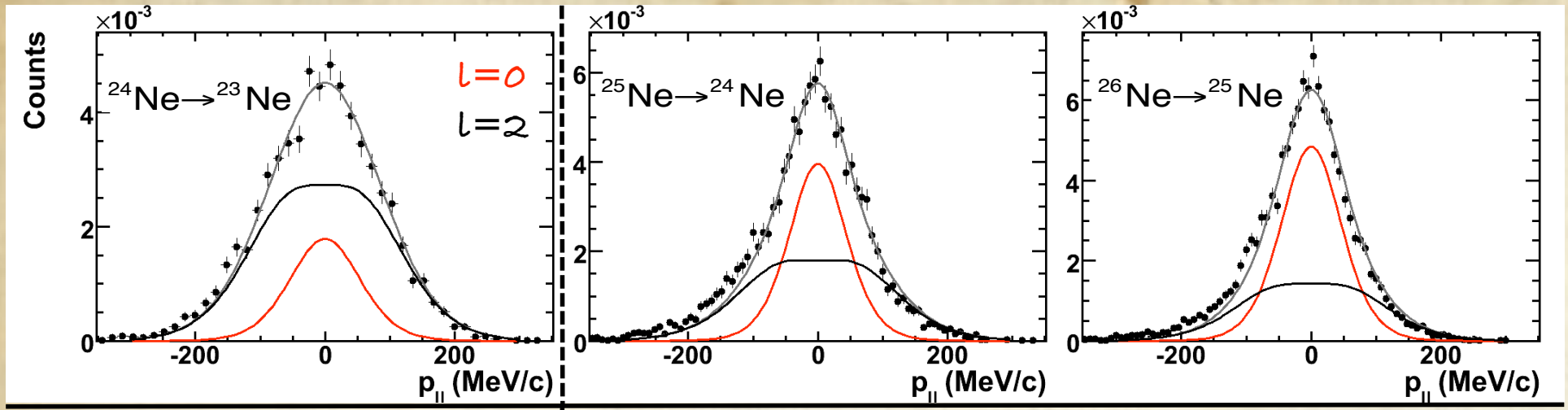

Transition from $d_{5/2}$ to $s_{1/2}$ configurations at N=15

Projectile	Fragment	l	Weight
^{24}Ne (0^+)	^{23}Ne ($5/2^+$, gs)	2	0.74 ± 0.05
	^{23}Ne ($1/2^+$, 1017)	0	0.25 ± 0.05
^{25}Ne ($1/2^+$)	^{24}Ne (0^+, gs)	0	0.46 ± 0.03
	^{24}Ne (2^+, 1982)	2	0.51 ± 0.03
^{26}Ne (0^+)	^{25}Ne ($1/2^+$, gs)	0	0.59 ± 0.03
	^{25}Ne ($5/2^+$, 1703)	2	0.38 ± 0.03

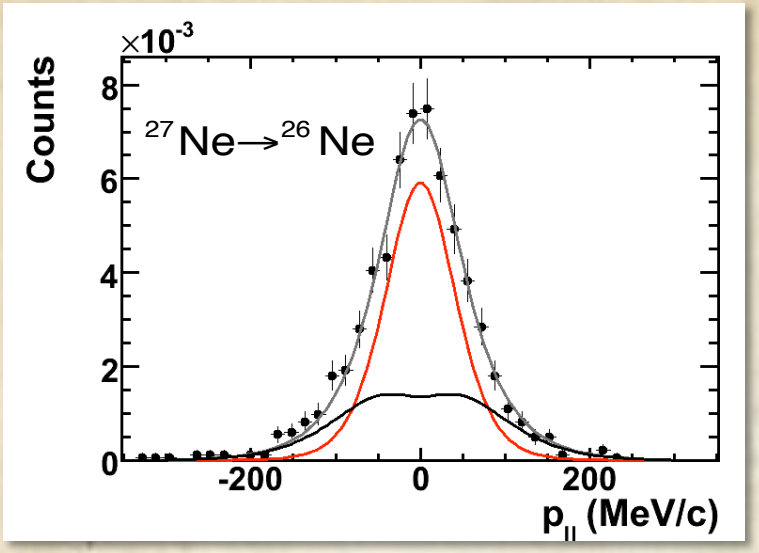

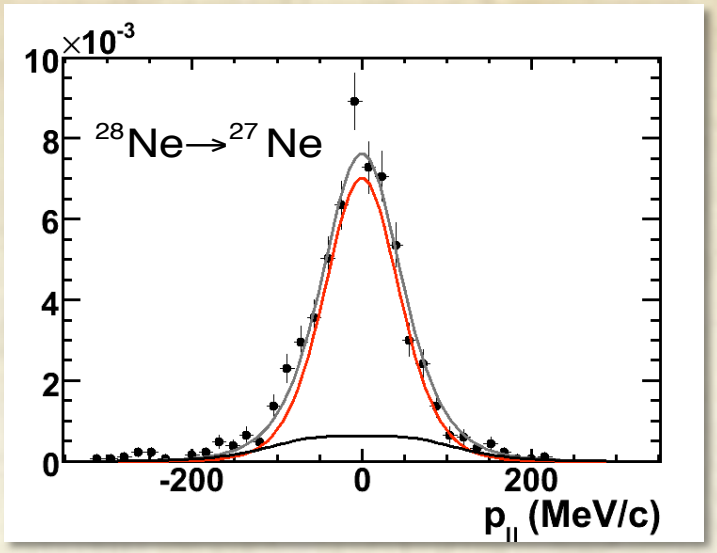

l=0
l=2

The last neutron occupies a $s_{1/2}$ level, rather than $d_{3/2}$, and is coupled to an excited state of the core.

Projectile	Fragment	l	Weight
^{27}Ne ($3/2^+$)	^{26}Ne (0^+, gs)	2	0.34 ± 0.11
	^{26}Ne (2^+, 2024)	0	0.64 ± 0.12
^{28}Ne (0^+)	^{27}Ne ($3/2^+$, gs)	2	0.16 ± 0.08
	^{27}Ne ($1/2^+$, 885)	0	0.81 ± 0.09

C. Rodriguez-Tajes et al., Phys. Lett. B 687 (2010) 26.

A previous knockout experiment for ^{26,28}Ne

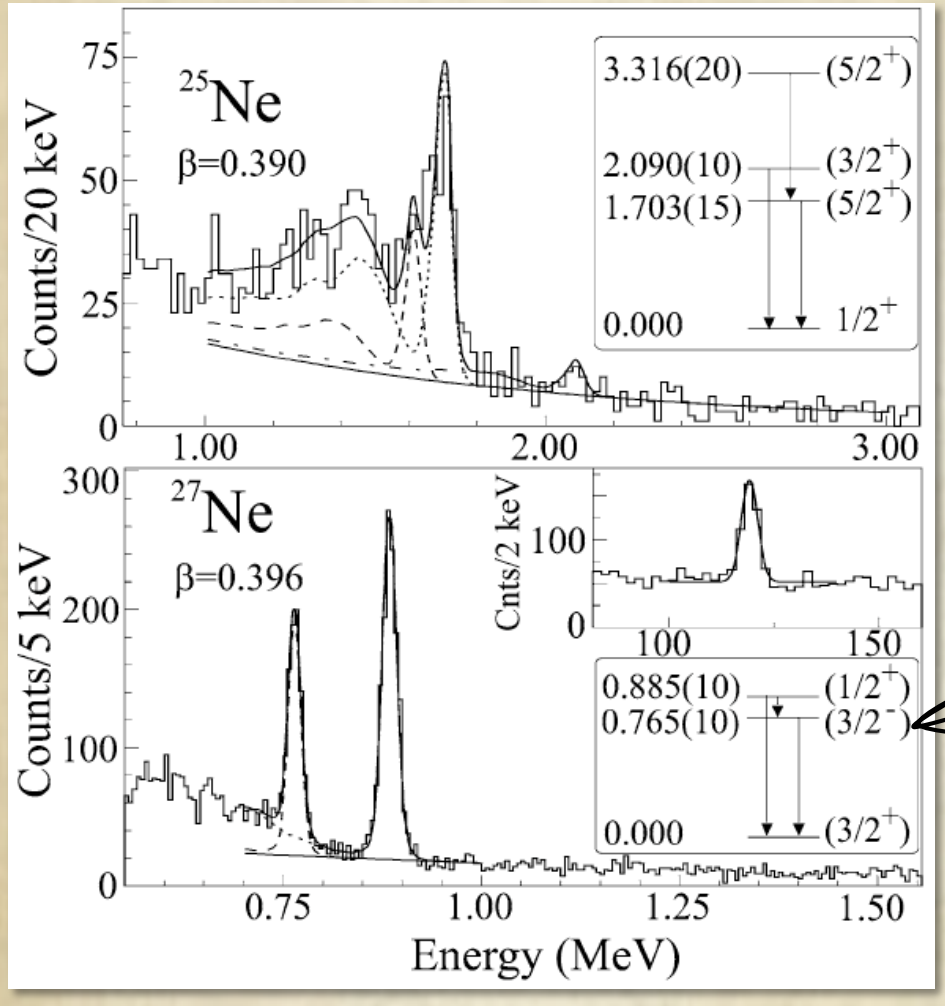

In agreement with USD and SDPF-M

Only predicted by SDPF-M (intruder state).

Terry et al., Phys. Lett. B 640 (2006) 86.

Our results agree with Terry et al. for the population of the ground state of the core (difference of 16%).

Conclusions

-Thirty-nine nuclei, from C to Al and with N=9-22, have been experimentally studied.

-Two inclusive observables: $p_{||}$ and σ_{-n}, were determined and exclusive measurements were carried out for ^{17}C and ^{19}N (also for ^{21}O and ^{25}F).

- One-neutron halo configurations in odd-mass C isotopes.
- Results for N, O, F and Ne isotopes reflect the change from $d_{5/2}$ to $s_{1/2}$ configurations at N = 15.
- First one-neutron knockout data for ^{22}N (one-neutron halo candidate).
- The ground state of ^{27,28}Ne is dominated by excited states of the core coupled to a $s_{1/2}$ neutron.

- Further study of exclusive data would provide detailed spectroscopic information.

The S245 Collaboration

C. Rodríguez-Tajes[1], D. Cortina-Gil[1], H. Álvarez-Pol[1], E. Benjamim[1], J. Benlliure[1], M. J. G. Borge[2], M. Caamaño[1], E. Casarejos[1], A. Chatillon[3], K. Eppinger[4], T. Faestermann[4], M. Gascón[1], H. Geissel[3], R. Gernhäuser[3], B. Jonson[5], R. Krücken[3], T. Kurtukian[1], P. Maierbeck[3], T. Nilsson[5], C. Nociforo[3], C. Pascual-Izarra[2], A. Perea[2], D. Pérez-Loureiro[1], A. Prochazka[3], H. Simon[3], K. Sümmerer[3], O. Tengblad[2], H. Weick[3], M. Zhukov[5]

[1]Universidade de Santiago de Compostela (Spain).
[2]Instituto de estructura de la materia, CSIC (Spain).
[3]GSI Helmholzzentrum für Schwerionenforschung (Germany).
[4]Technische Universität München (Germany).
[5]Chalmers Tekniska Högskola och Göteborgs Universitet (Sweden).

Acceptance cuts

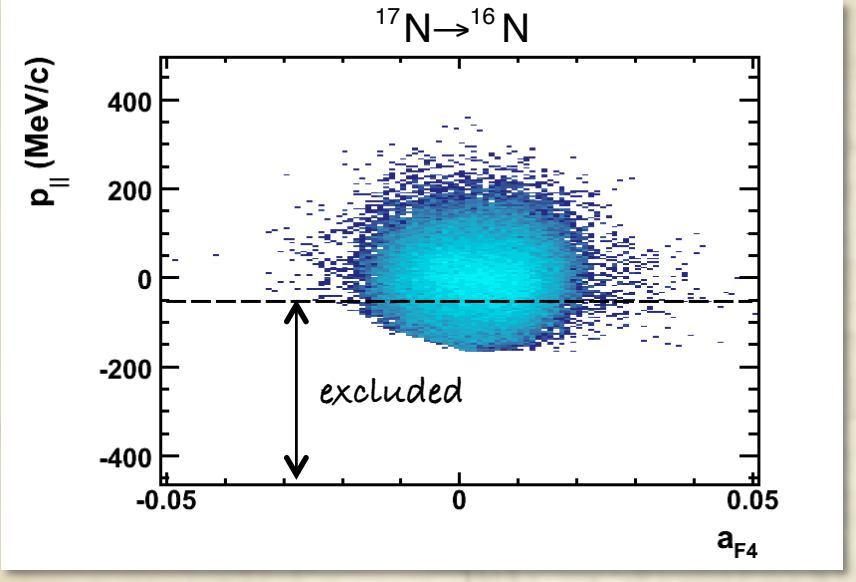

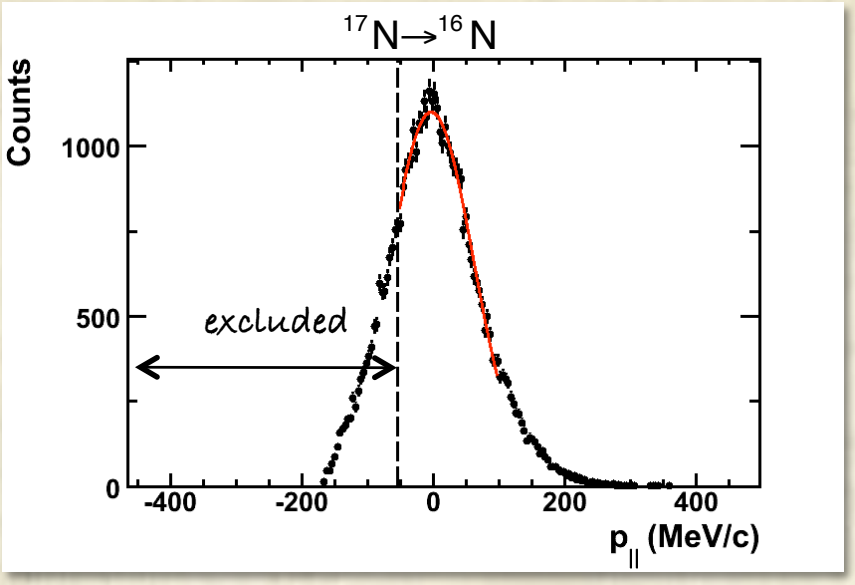

Artificial cuts appeared for those cases close to the acceptance limits of the FRS.

Momentum resolution

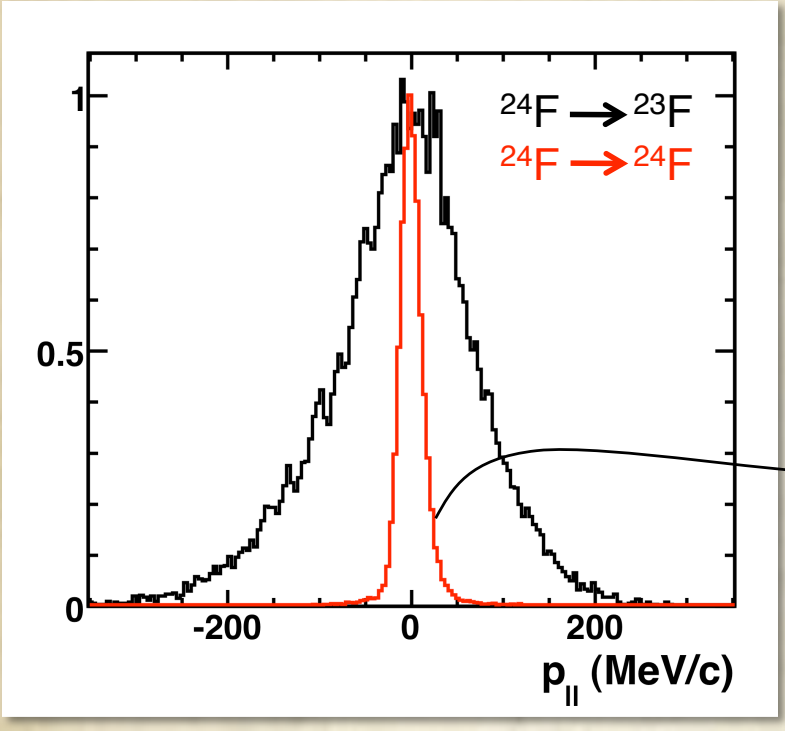

Measurement of projectiles that did not react in the target.

The width was corrected from the momentum resolution.

$$FWHM_{corrected} = \sqrt{FWHM^2_{^{24}F^{23}F} - FWHM^2_{^{24}F^{24}F}}$$

Comparison with previous experiments ($p_{||}$)

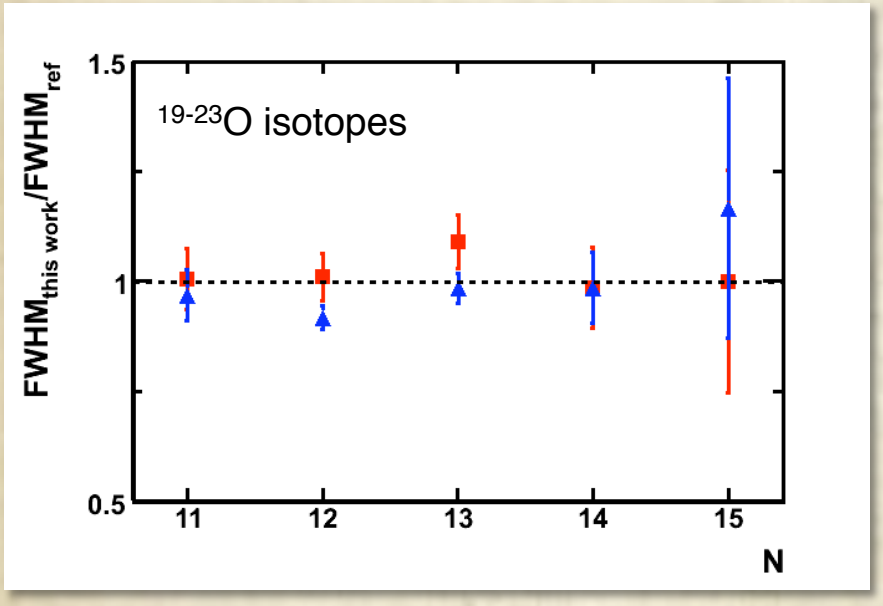

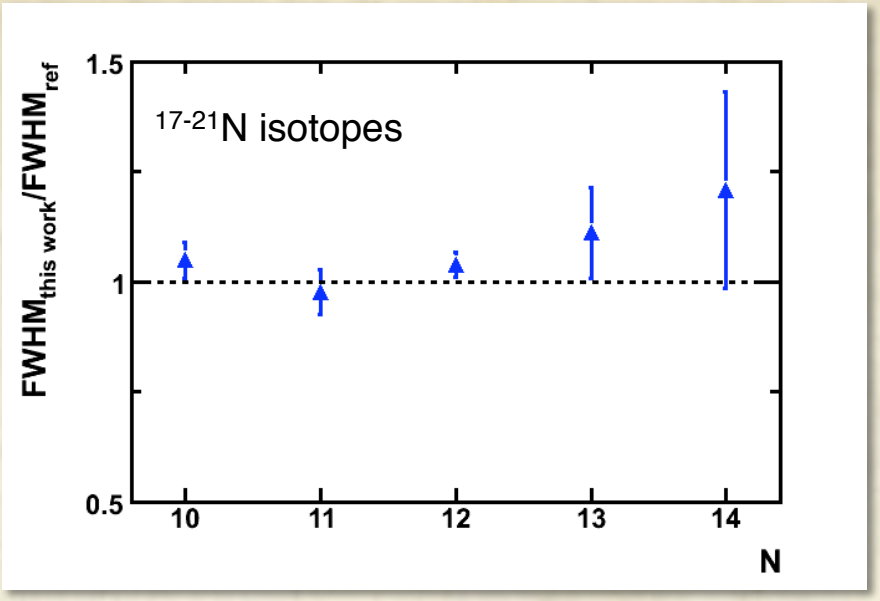

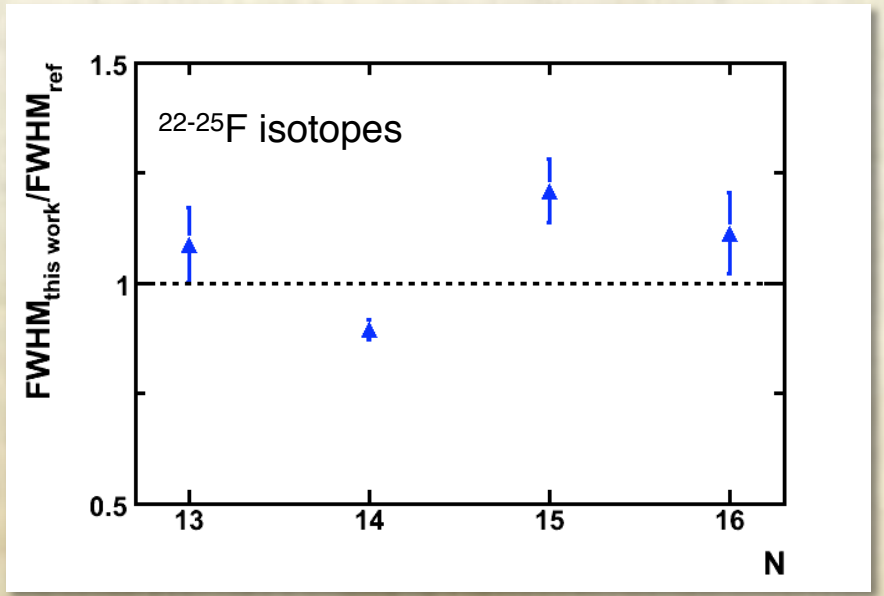

Cortina et al., Phys. Rev. Lett. 93 (2004) 062501.

Sauvan et al., Phys. Rev. C 69 (2004) 044603.

Comparison with previous experiments (σ_{-n})

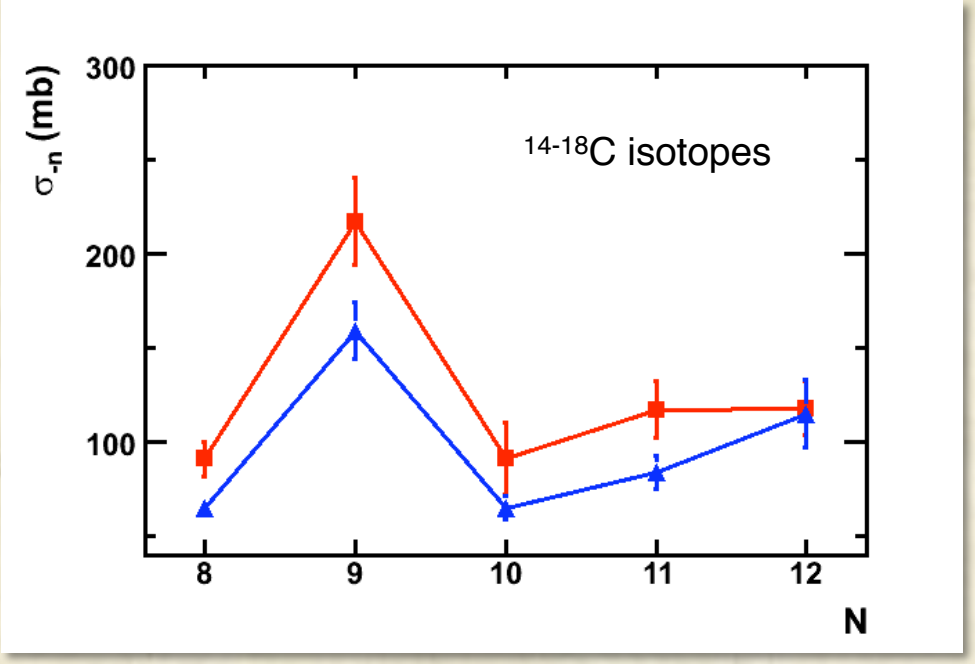

This work.

Sauvan et al., Phys. Rev. C 69 (2004) 044603.

^{21}O one-neutron knockout

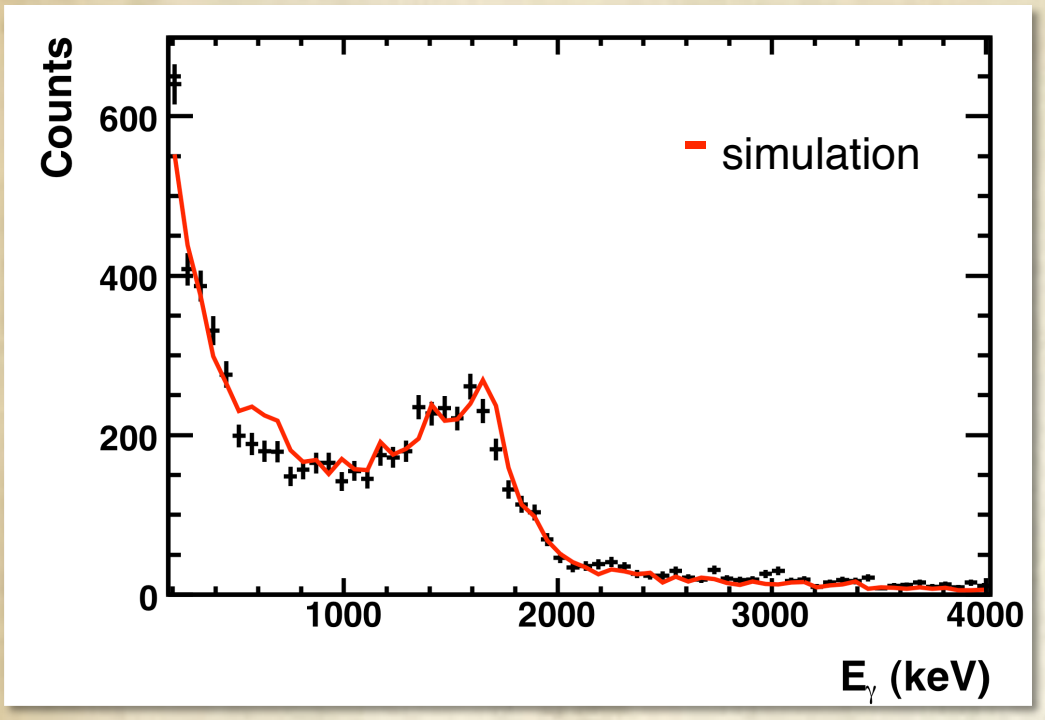

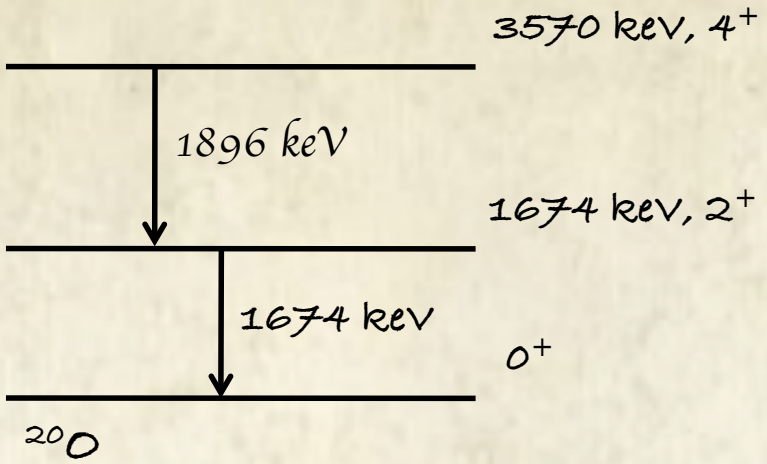

I^π	E (keV)	σ_{-n} (mb)	b
0^+	0	21 ± 5	0.28 ± 0.06 0.53 (i)
2^+	1674	36 ± 6	0.48 ± 0.04 0.09 (i)
4^+	3570	18 ± 4	0.24 ± 0.04 0.38 (i)

Our conclusions contradict the work of Fernández et al., PhD thesis.

(i) Fernández PhD thesis, USC 2003.

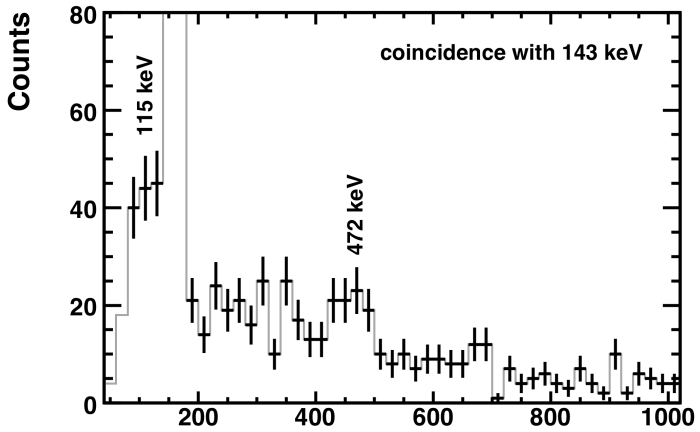

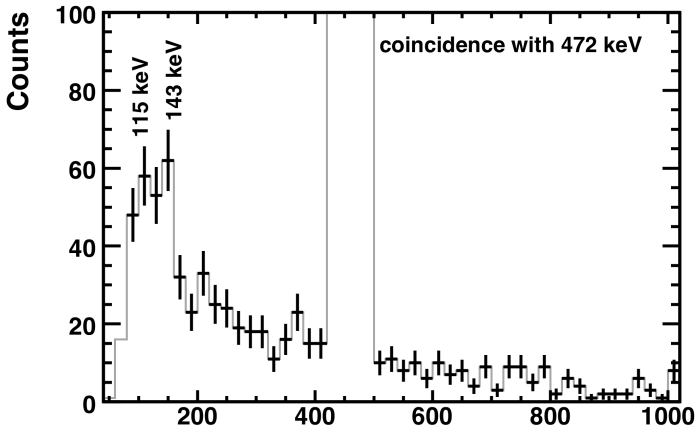

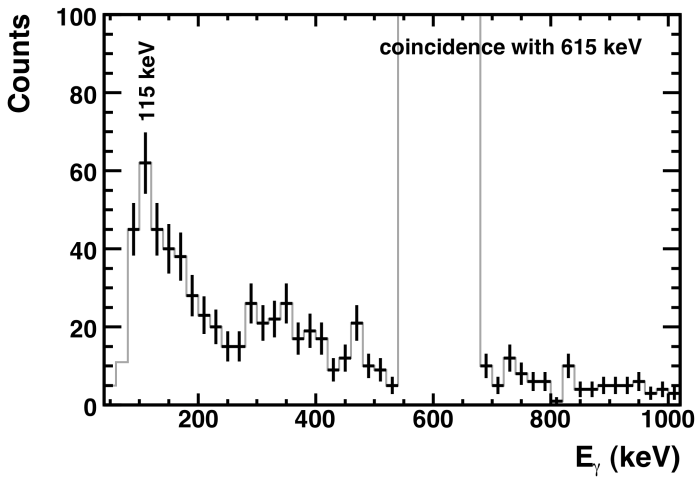

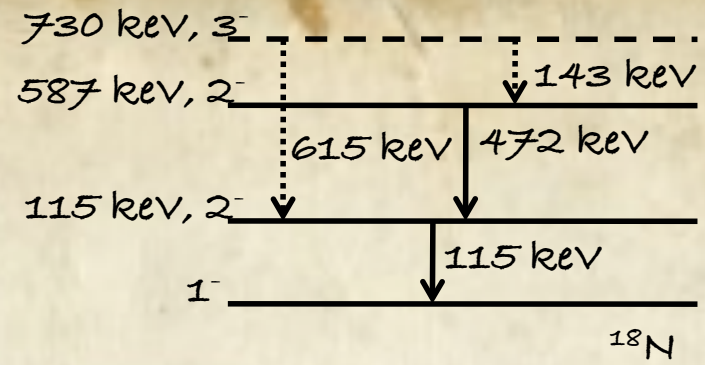

In agreement with Wiedeking et al.

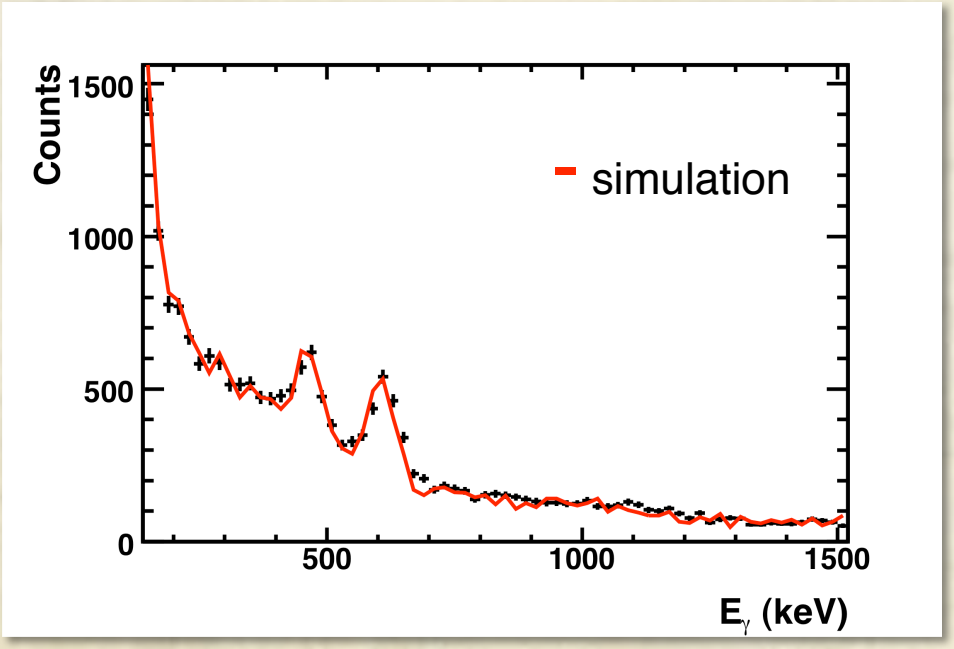

I^π	E (keV)	σ_{-n} (mb)	b
2^-	587	$< 6 \pm 2$	$< 0.09 \pm 0.02$
3^-	730	$> 15 \pm 2$	$> 0.23 \pm 0.01$

^{25}F one-neutron knockout

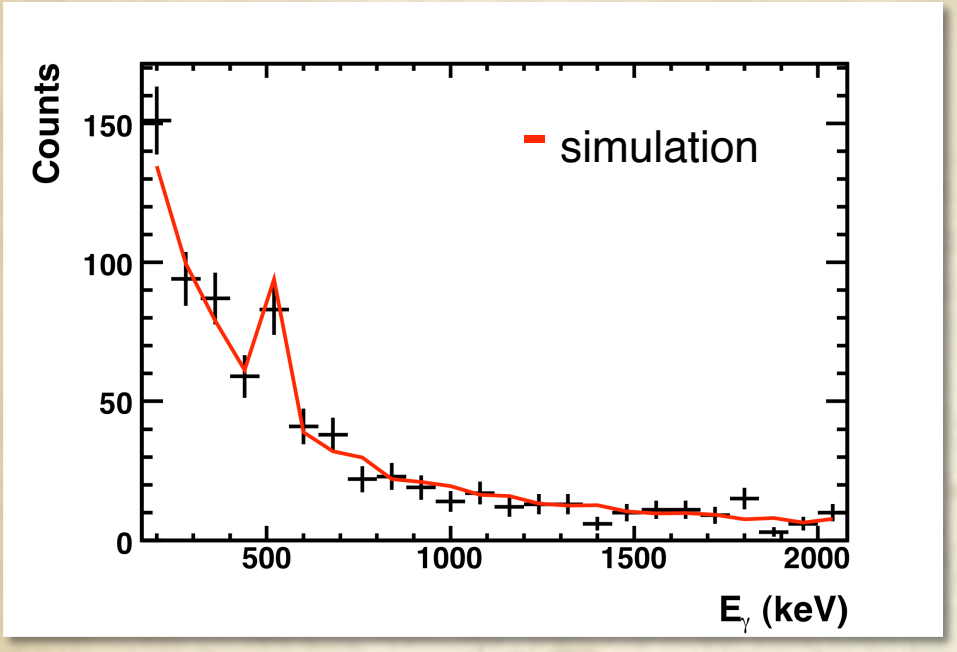

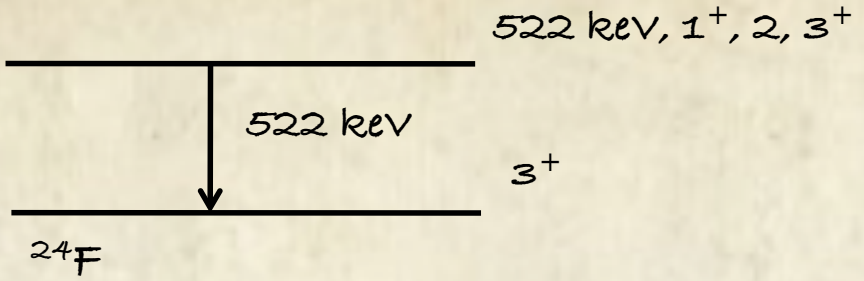

The first excitation level of ^{24}F was populated in the reaction.

Exclusive measurements performed for the first time in ^{25}F one-neutron knockout.

I^π	E (keV)	σ_{-n} (mb)	b
3^+	0	59 ± 12	0.85 ± 0.03
$1^+, 2, 3^+$	522	10 ± 3	0.15 ± 0.03

Geant4 simulation of MINIBALL

velocity of emitting nucleus beta = 0.707

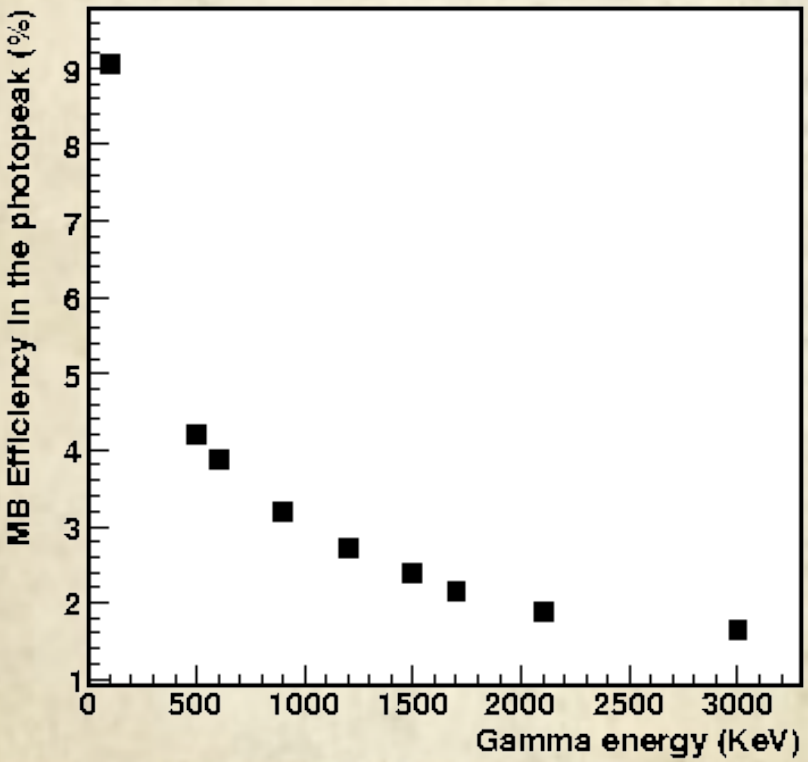

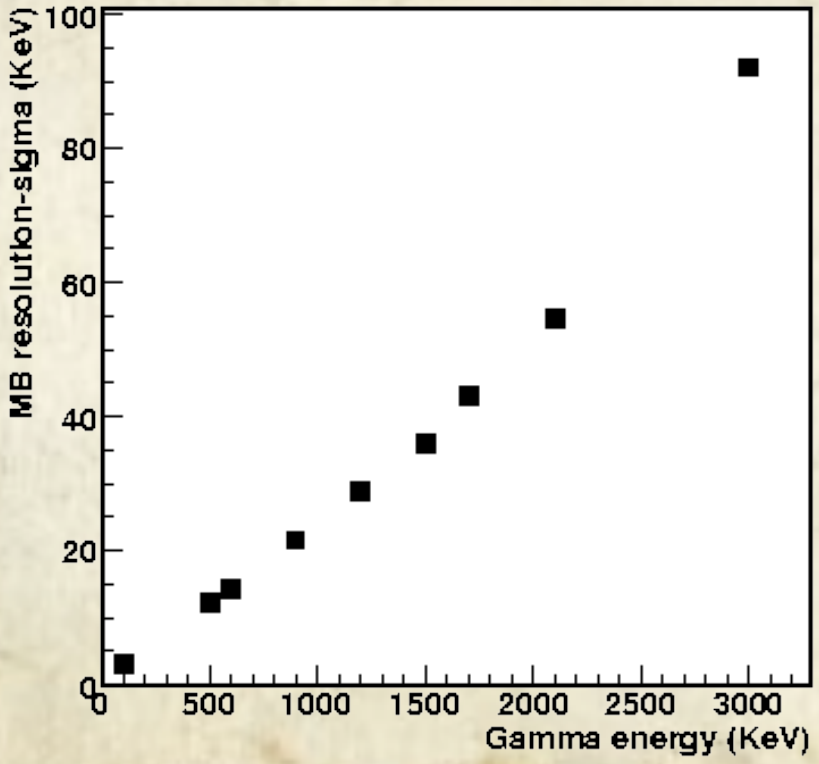

Efficiency in γ measurements

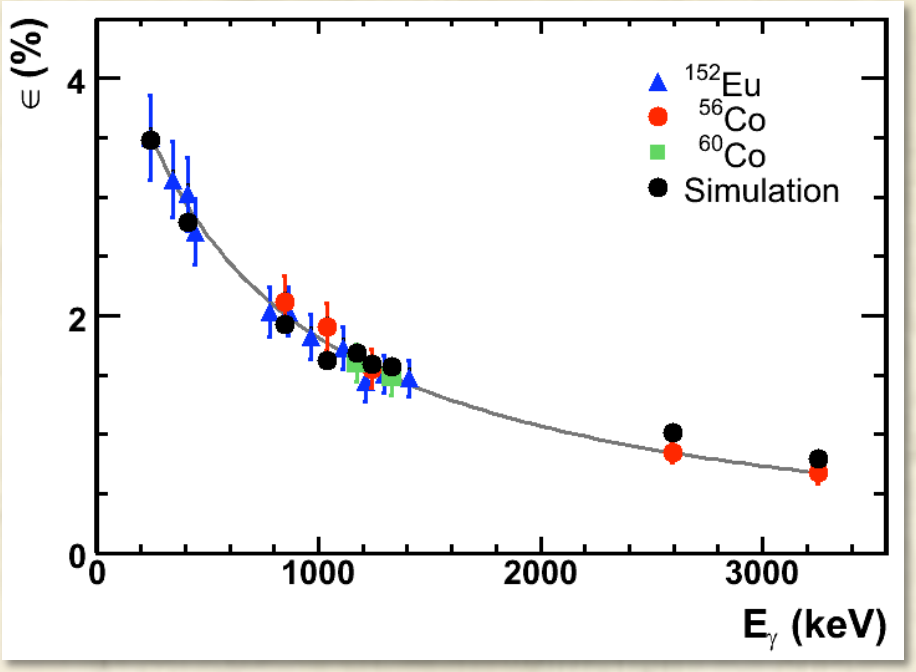

The MINIBALL detection efficiency was calculated with a Geant 4 simulation.

The dead time of the detector and the efficiency of the acquisition module were also taken into account.